

# Enhanced Seebeck coefficient through the magnetic fluctuations in $\text{Sr}_2\text{Ru}_{1-x}\text{M}_x\text{O}_4$ ( $M = \text{Co}, \text{Mn}$ )

Takayoshi Yamanaka,\* Ryuji Okazaki,† and Hiroshi Yaguchi  
Department of Physics, Faculty of Science and Technology,  
Tokyo University of Science, Noda, Chiba 278-8510, Japan  
(Dated: May 12, 2022)

The layered perovskite  $\text{Sr}_2\text{RuO}_4$  is a most intensively studied superconductor, but its pairing mechanism, which is often coupled intimately with magnetic fluctuations in correlated materials, is still an open question. Here we present a systematic evolution of the Seebeck coefficient in Co- and Mn-substituted  $\text{Sr}_2\text{RuO}_4$  single crystals, in which ferromagnetic and antiferromagnetic glassy states respectively emerge in proximity to the superconducting phase of the parent compound. We find that the Seebeck coefficient  $S$  divided by temperature  $T$ ,  $S/T$ , shows a maximum near characteristic temperatures seen in the irreversible magnetization  $M_{\text{ir}}$  in both of the Co- and Mn-substituted crystals, demonstrating both of the ferromagnetic and antiferromagnetic fluctuations to enhance the Seebeck coefficient. Interestingly,  $S/T$  increases with lowering temperature in the parent compound, reminiscent of non-Fermi-liquid behavior, indicating an essential role of coexisting ferromagnetic and antiferromagnetic fluctuations for the itinerant electrons in  $\text{Sr}_2\text{RuO}_4$ .

## I. INTRODUCTION

Unconventional superconductivity in the layered perovskite  $\text{Sr}_2\text{RuO}_4$  has long attracted interest [1–6]. In particular, recent progress of nuclear magnetic resonance (NMR) experiments has posed strong constraints on the spin sector of the superconducting order parameter [7–9], offering a clue for the consistent understanding of several experimental results [10–12] that were difficult to reconcile with earlier NMR results [13–16], as well as stimulating further symmetry-based experiments to elucidate the order parameter [17–19]. As a result, an exotic two-component order parameter with broken time reversal symmetry has been proposed, which is unique as suggested in several examples [20, 21], and various theoretical attempts have also been made [22–27], opening an avenue for exploring unconventional pairing interaction to realize such order parameters.

To address this underlying issue, it is crucially important to establish the electronic phase diagram as a function of external parameters such as pressure and chemical substitutions, as is widely discussed in correlated matters [28, 29]. Indeed, although the superconducting state in  $\text{Sr}_2\text{RuO}_4$  is extremely sensitive to impurity [30], dramatic changes in the electronic state with elemental substitutions have been reported. In the isovalent systems, for instance, a spin-glass state develops over a wide range of the Ca content in  $(\text{Sr}, \text{Ca})_2\text{RuO}_4$  [31, 32], which may originate from the degree of freedom in the  $\text{RuO}_6$  octahedra. On the other hand, in  $\text{Sr}_2(\text{Ru}, \text{Ti})\text{O}_4$ , an incommensurate spin-density-wave ordering due to the Fermi-surface nesting appears with glassy behavior [33]. In contrast to the antiferromagnetic (AFM) coupling seen in the isovalent systems,  $\text{La}^{3+}$  substitution to  $\text{Sr}^{2+}$  sites results in electron doping to expand the electron-like  $\gamma$  Fermi surface, leading to ferromagnetic (FM) fluctuation owing to an enhancement of the density of states (DOS) at the Fermi energy  $N(\epsilon_F)$  near the van Hove singularity (vHs) [34–36]. These results clearly show the complicated magnetic instabilities existing in the parent compound  $\text{Sr}_2\text{RuO}_4$ , which involve complex structural and electronic origins. Such instabilities are also discussed in sev-

eral studies including NMR and neutron experiments [37–41].

Among many substituted systems, Co- and Mn-substituted  $\text{Sr}_2\text{RuO}_4$  serve as a fascinating platform to investigate how magnetic fluctuations mediate the emergence of superconductivity, because slight substitutions of Co and Mn drastically vary the superconducting ground state into the FM and AFM glassy states, respectively [42]. In the Co-substituted system, the FM cluster glass characterized by an exponential relaxation of the remanent magnetization appears at low temperatures. Also, the electronic specific heat  $\gamma_e$  increases with increasing Co contents, indicating an increased  $N(\epsilon_F)$  similar to La-substitution [34]. It is noteworthy that the increase of  $N(\epsilon_F)$  in a 1.5% Co-substituted sample estimated from  $\gamma_e$  is comparable to that in a 5% La-substituted sample, possibly implying an effective electron doping effect by the Co substitution [42]. Similarly, the AFM transition temperature in Mn-substituted samples is much higher than that in Ti-substituted ones, demonstrating enigmatic roles of the Co and Mn substitutions to strengthen the magnetic couplings in  $\text{Sr}_2\text{RuO}_4$ .

The aim of this study is to examine such magnetic fluctuations in  $\text{Sr}_2\text{Ru}_{1-x}\text{M}_x\text{O}_4$  ( $M = \text{Co}, \text{Mn}$ ) by means of Seebeck coefficient measurement, known as a powerful tool for fluctuations as it is a measure of the entropy per charge carrier [43]. The observed temperature dependence of  $S/T$  ( $S$  and  $T$  being the Seebeck coefficient and temperature, respectively) has a maximum near characteristic temperatures in the magnetization in both Co- and Mn-substituted samples, indicating that both FM and AFM fluctuations are responsible for the enhancement of the Seebeck coefficient. Moreover, in sharp contrast to the typical metallic behavior in which  $S/T$  remains constant,  $S/T$  increases with cooling in the parent compound, implying both FM and AFM fluctuations remaining in the itinerant electrons in  $\text{Sr}_2\text{RuO}_4$ .

## II. EXPERIMENTAL DETAILS

Single crystals of  $\text{Sr}_2\text{Ru}_{1-x}\text{M}_x\text{O}_4$  ( $M = \text{Co}, \text{Mn}$ ) were grown by a floating-zone method using an image furnace

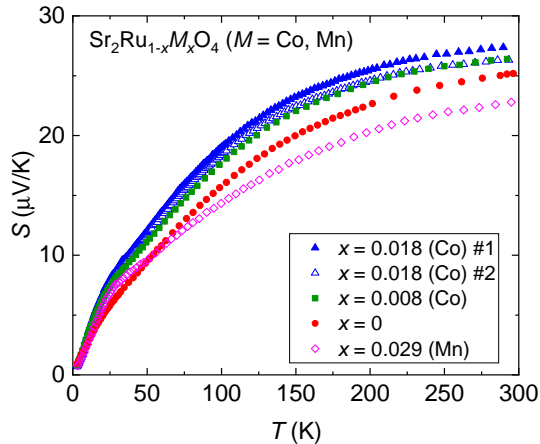


FIG. 1. Temperature dependence of the Seebeck coefficient  $S$  of  $\text{Sr}_2\text{Ru}_{1-x}\text{M}_x\text{O}_4$  ( $M = \text{Co}, \text{Mn}$ ) single crystals.

with a pair of halogen lamps and elliptical mirrors [42, 44]. We used high-purity  $\text{SrCO}_3$  (99.99%+),  $\text{RuO}_2$  (99.9%),  $\text{MnO}_2$  (99.99%), and  $\text{CoO}$  (99.9%) as starting materials. An excess 15% amount of  $\text{RuO}_2$  was weighed to compensate for evaporation of Ru during single crystal growth. The concentration of Mn and Co in obtained crystals were determined by electron probe micro analyzer. The measured Mn concentration was 2.9%, well corresponding to the nominal concentration of 3%. In contrast, the measured Co concentrations were 1.8% and 0.8% for nominally 3% and 1% Co-substituted samples, respectively. The relation between the nominal and measured concentrations is consistent with the trend reported in Ref. 42.

The typical dimension of the measured crystals was  $\approx 3 \times 0.2 \times 0.2 \text{ mm}^3$ . The Seebeck coefficient was measured by a steady-state technique using a manganin-constantan differential thermocouple in a closed-cycle refrigerator. The thermoelectric voltage of the sample was measured with Keithley 2182A nanovoltmeter. The temperature gradient with a typical temperature gradient of 0.5 K/mm was applied along the  $ab$ -plane direction using a resistive heater. The thermoelectric voltage from the wire leads was subtracted. Magnetization was measured using a superconducting quantum interference device magnetometer (Quantum Design, MPMS) under field-cooled (FC) and zero-field-cooled (ZFC) processes with the external field of  $\mu_0 H = 0.1 \text{ T}$  applied along the  $c$  axis.

### III. RESULTS AND DISCUSSIONS

Figure 1 summarizes the temperature variations of the Seebeck coefficient  $S$  in  $\text{Sr}_2\text{Ru}_{1-x}\text{M}_x\text{O}_4$  ( $M = \text{Co}, \text{Mn}$ ) single crystals. Overall behavior of  $S$  in the parent compound  $\text{Sr}_2\text{RuO}_4$  is consistent with earlier results [45, 46], and is discussed as an intriguing example to study the internal degrees

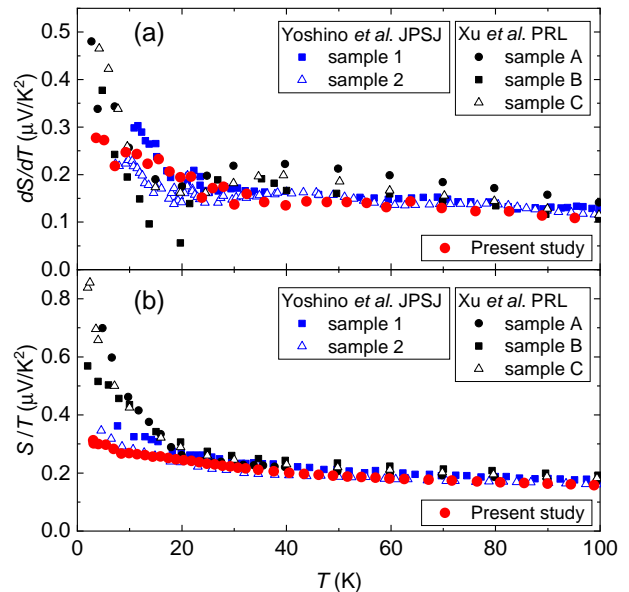


FIG. 2. Comparison of the temperature dependence of (a)  $dS/dT$  and (b)  $S/T$  of  $\text{Sr}_2\text{RuO}_4$  single crystals. The red circles show the present data, and the others are data extracted from Refs. 45 and 46.

of freedom in correlated metals [47]. In the substituted compounds,  $S$  increases (decreases) with Co (Mn) substitutions near room temperature probably because of the electron (hole) doping effect as suggested in Ref. 42.

In Refs. 45 and 46, the Seebeck coefficient in the parent compound was analyzed in the differential form  $dS/dT$ , and an anomaly was found near 20 – 25 K. Xu *et al.* have suggested that a band-dependent coherence is developed below the anomaly temperature on the basis of the results of the Seebeck and the Nernst measurements [46]. Indeed, such a coherency seems to be vital in this system [48]. To see this anomaly at 20 – 25 K, we compare the present data for  $\text{Sr}_2\text{RuO}_4$  with the results extracted from Refs. 45 and 46 in Fig. 2(a). Although there is a sample dependence in magnitude, all the data exhibit a kink around 20 – 25 K, in good agreement with the present result. Also note that the effect from the impurity phase of  $\text{SrRuO}_3$  is negligible, because the Seebeck coefficient  $S$  in a composite sample with the conductivity  $\sigma$  is given as  $\sigma S = \sum_k \alpha_k \sigma_k S_k$  in a parallel-circuit model, where  $\alpha_k, \sigma_k, S_k$  are the volume fraction, the conductivity, and the Seebeck coefficient for the material  $k$  [49], and the volume fraction of the impurity phase in the present crystal was negligibly small.

Here we discuss the Seebeck coefficient in the form of  $S/T$  instead of  $dS/dT$ , since the Seebeck coefficient in the free-electron model (oversimplified model to multiband  $\text{Sr}_2\text{RuO}_4$ ) is expressed as  $S \approx -\frac{k_B^2 T}{e} \frac{N(\mu)}{n}$ , where  $k_B, e, n, \mu,$  and  $N$  are the Boltzmann constant, elementary charge, carrier density, chemical potential, and the DOS, respectively [50]. In

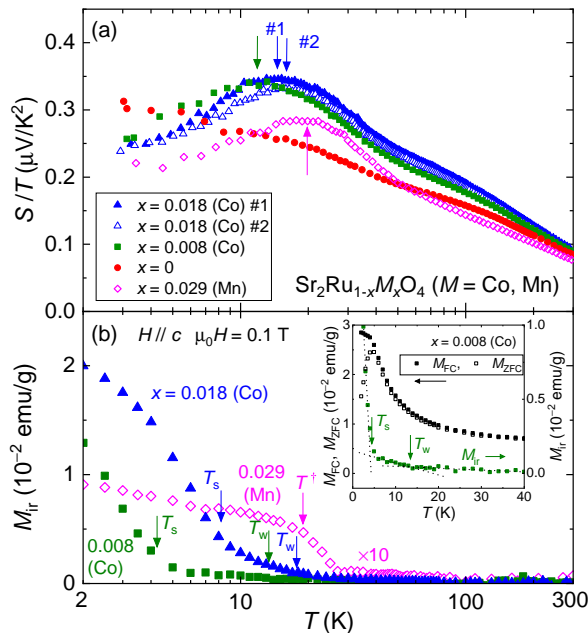


FIG. 3. (a) Temperature dependence of  $S/T$  of  $\text{Sr}_2\text{Ru}_{1-x}\text{M}_x\text{O}_4$  ( $M = \text{Co}, \text{Mn}$ ) single crystals. The arrows show the peak temperature  $T_{\text{peak}}$ . (b) Temperature dependence of the irreversible magnetization  $M_{\text{ir}} \equiv M_{\text{FC}} - M_{\text{ZFC}}$ . The arrows represent the characteristic temperatures  $T^\dagger$ ,  $T_s$ , and  $T_w$ . (See text for details.) In the inset,  $M_{\text{FC}}$ ,  $M_{\text{ZFC}}$ , (left axis) and  $M_{\text{ir}}$  (right axis) of the 0.8% Co-substituted sample are shown together with the definitions of  $T_s$  and  $T_w$ .

this form, one can follow the temperature dependence of the DOS or carrier density, as is widely analyzed in correlated electron systems, similar to the case of the pseudogap state in transition-metal oxides [51–53] and heavy-fermion formation in rare-earth compounds [54]. Note that the differential  $dS/dT$  includes the temperature derivatives of  $N(\mu)$  and  $n$  in complicated forms. Figure 2(b) represents the temperature dependence of  $S/T$  in  $\text{Sr}_2\text{RuO}_4$  in the present crystals and the calculated  $S/T$  from the extracted data from Refs. 45 and 46. Interestingly, all the data are temperature-dependent; in sharp contrast to conventional metals, in which  $S/T$  remains constant [43],  $S/T$  significantly increases with decreasing temperature, the origin of which will be discussed later.

We then focus on the temperature variation of  $S/T$  in the substituted systems. Figure 3(a) represents the temperature dependence of  $S/T$  in  $\text{Sr}_2\text{Ru}_{1-x}\text{M}_x\text{O}_4$  ( $M = \text{Co}, \text{Mn}$ ), in which we find a drastic change due to substitutions. At low temperatures,  $S/T$  exhibits a prominent peak structure in the temperature dependence for both substituted systems. The peak temperature  $T_{\text{peak}}$  defined as the temperature at which  $S/T$  exhibits a maximum is shown by arrows in Fig. 3(a). Note that the phonon-drag effect is unlikely to enhance the Seebeck coefficient in the substituted systems, because the substitutions generally suppress the phonon mean free path [55].

To shed light on the relation to the magnetism, we plot the irreversible magnetization  $M_{\text{ir}}$  defined as  $M_{\text{ir}} \equiv M_{\text{FC}} - M_{\text{ZFC}}$ , in Fig. 3(b). ( $M_{\text{FC}}$  and  $M_{\text{ZFC}}$  being the magnetization measured under FC and ZFC processes, respectively). While the onset of the irreversibility may correspond to a transition to the FM and AFM glassy states for the Co- and Mn-substituted systems, respectively [42], a close look of the  $M_{\text{ir}}$  data reveals that the onset of the irreversibility is accompanied by a double step. The inset of Fig. 3(b) shows the temperature variations of  $M_{\text{FC}}$ ,  $M_{\text{ZFC}}$ , and  $M_{\text{ir}}$  for  $x = 0.008$  (Co) at low temperatures. The  $M_{\text{ZFC}}$  data more steeply decrease than that in Ref. 42, but this may be due to the low applied field in our measurement. From the plots of  $M_{\text{ir}}$  in the inset, one can see that a weak irreversibility sets in at  $T_w \approx 14$  K and subsequently the irreversibility is strongly enhanced below  $T_s \approx 4$  K. The weak and strong irreversibility temperatures  $T_w$  and  $T_s$  are defined as the points of intersection of the two linear lines as drawn in the dotted line in the inset. Importantly, such a co-existence of weak and strong irreversibility is often observed in ferromagnetic spin-glass systems [56–59], and theoretically interpreted in terms of a multi component vector spin model given by Gabay and Toulouse [60], in which the transverse spin components are first frozen at  $T_w$  on cooling and then followed by the freezing of the longitudinal spin components at  $T_s$ , although it is still under debate whether it represents a true thermodynamic phase transition.

On the other hand, the temperature dependence of  $M_{\text{ir}}$  in the Mn-substituted sample is different from that in the Co-substituted samples: On cooling, the irreversibility sets in at  $T \approx 27$  K, which is almost identical to the onset temperature  $T_{\text{ir}}$  to the static order [42], and then shows weak temperature dependence below  $T^\dagger \approx 18$  K at which  $M_{\text{ir}}$  displays a kink structure as shown in Fig. 3(b). In the Mn-substituted sample,  $T_{\text{peak}}$  in  $S/T$  is close to this anomaly temperature  $T^\dagger$ , although the origin of  $T^\dagger$  is unclear at present. Note that the remanent magnetization is also distinct among the Co- and Mn-substituted systems: While the temperature dependence of remanent magnetization is monotonic in the Co-substituted samples, it exhibits an anomalous peak structure below the onset temperature  $T_{\text{ir}}$  for the Mn-substituted systems [42], implying the existence of a characteristic temperature below  $T_{\text{ir}}$ . The nature of the magnetic glassy state is an issue for the future study using the microscopic NMR and neutron measurements.

In Fig. 4, we plot the peak temperature  $T_{\text{peak}}$  in  $S/T$  together with  $T_s$ ,  $T_w$ , and  $T^\dagger$  on the phase diagram reported in Ref. 42. The peak temperature  $T_{\text{peak}}$  in  $S/T$  well coincides with the weak irreversibility temperature  $T_w$  and the anomaly temperature  $T^\dagger$  for the Co- and Mn-substituted samples, respectively, indicating an intimate relationship among the Seebeck coefficient and the magnetic fluctuations. Here, since the Co and Mn substitutions induce the FM cluster glass and the spin glass states with short-range AFM order, respectively [42], the present results indicate that both FM and AFM fluctuations are substantial for the enhancement of the Seebeck coefficient at  $T_{\text{peak}}$ . Indeed, it bears a striking resemblance to

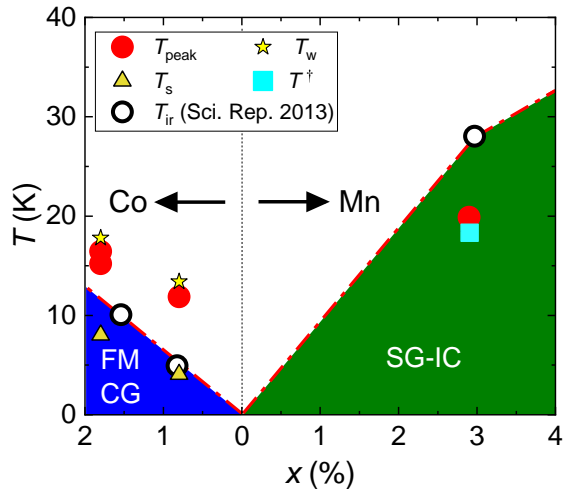


FIG. 4. Phase diagram of  $\text{Sr}_2\text{Ru}_{1-x}\text{M}_x\text{O}_4$  ( $M = \text{Co}, \text{Mn}$ ). The closed circles shows the peak temperature  $T_{\text{peak}}$  at which  $S/T$  exhibits maximum. The weak and strong irreversibility temperatures  $T_w$  (stars) and  $T_s$  (triangles) and the anomaly temperature  $T^\dagger$  (square) are determined from the irreversibility magnetization  $M_{\text{ir}}$ . The onset temperature  $T_{\text{ir}}$  (open circles) and the regions of FM cluster glass (CG) and spin glass state with short-range incommensurate AFM order (SG-IC) are extracted from Ref. 42.

that in the itinerant magnets such as the perovskite ruthenate  $\text{CaRu}_{0.8}\text{Sc}_{0.2}\text{O}_3$  [61] and the doped Heusler alloy  $\text{Fe}_2\text{VAl}$  [62]; in these compounds, the Seebeck coefficient is enhanced near the ferromagnetic transition temperature through a sort of the magnon-drag effect, and is reduced by applying magnetic field owing to the field-induced suppression of the magnetic fluctuation. In the antiferro-quadrupole (AFQ)  $\text{PrIr}_2\text{Zn}_{20}$ , moreover,  $S/T$  exhibits a peak structure near the AFQ transition temperature in high magnetic field where the quadrupolar fluctuation could be enhanced [63].

Now let us recall the  $S/T$  behavior in  $\text{Sr}_2\text{RuO}_4$  (Fig. 2), which increases with cooling down to the lowest temperature of the present measurement ( $\sim 3$  K). While Seebeck coefficients are not strictly linear in temperature even in simple metals [64], the non-linearity in  $\text{Sr}_2\text{RuO}_4$  is unusual. As mentioned above, we show the suggestive evidence that both FM and AFM fluctuations drive the enhanced Seebeck coefficient in the vicinity of the parent compound. It is therefore reasonable to consider that, even in the parent compound  $\text{Sr}_2\text{RuO}_4$ ,  $S/T$  is enhanced similarly down to zero temperature, at which both FM and AFM glassy states tend to terminate for  $\text{Sr}_2\text{RuO}_4$  [42]. Thus this is a kind of non-Fermi-liquid (NFL) behavior close to the quantum critical point [65], which has also been observed in various correlated matters such as heavy fermions [66–70] and oxides [71]. Quite intriguingly, in contrast to the aforementioned systems, both FM and AFM fluctuations seem to be substantial for the itinerant electrons in  $\text{Sr}_2\text{RuO}_4$  as seen in the pronounced peak of  $S/T$  observed in both Co- and Mn-substituted compounds.

One may, however, pose a simple question regarding the specific heat. In  $\text{Sr}_2\text{RuO}_4$ , the electronic specific heat shows conventional Fermi-liquid (FL) behavior [72], in distinction to the NFL behavior observed in the Seebeck coefficient; since the Seebeck coefficient is also given as the specific heat per carrier [50], both quantities are expected to show similar anomalies [73]. On the other hand, an AFM quantum criticality may affect the ratio of these quantities in zero-temperature limit [74]. It is interesting to note that this effect of the AFM quantum criticality may be enhanced by the multi-band nature; in  $\text{Sr}_2\text{RuO}_4$ , the Fermi surfaces are composed of three cylindrical sheets: hole-like  $\alpha$  and electron-like  $\beta$  and  $\gamma$  sheets with the order of magnitudes of the effective mass of  $m_\alpha < m_\beta < m_\gamma$  [75–78]. Since the lighter band contributes to the transport more significantly in general [20, 79], the lighter  $\alpha$  and  $\beta$  bands are essential here, and importantly, these  $\alpha$  and  $\beta$  sheets possess the AFM instability due to nesting [38–41]. This band-dependent magnetic fluctuation may give origin to the anomalous low-temperature increase in  $S/T$ . On the other hand, it is unclear at present how the thermoelectric transport is affected by the FM fluctuation, the importance of which is clearly demonstrated in the Co-substituted systems; the existence of FM fluctuation is indicated by NMR [37], while the neutron experiments have revealed that it is very weak [38–41].

It is also known that the electrical resistivity of  $\text{Sr}_2\text{RuO}_4$  is well described within the FL scheme [72], in which the resistivity is given as  $\rho(T) = \rho_0 + AT^\nu$  with the exponent  $\nu = 2$ . On the other hand, the determination of  $\nu$  is delicate [80], and as seen in other correlated materials,  $\nu$  apparently depends on the residual resistivity even in high-purity level [81]. It may be useful to examine the exponent in high-purity crystals [82]. We also mention that the thermal conductivity in the normal state is interesting in the sense that it also mirrors the entropy flow, while the earlier studies are mainly devoted to the superconducting state [83–85]. Also, the Seebeck coefficient in the system with the Fermi level at the vHs, which is not achieved with the present Co substitution, is worth exploring because the topological change in the Fermi surface at vHs may lead to the significant enhancement of the Seebeck coefficient [86, 87]. This effect of the vHs could be investigated in electron-doped  $\text{Sr}_{2-x}\text{La}_x\text{RuO}_4$ .

#### IV. CONCLUSION

To summarize, we performed Seebeck coefficient measurement in  $\text{Sr}_2\text{Ru}_{1-x}\text{M}_x\text{O}_4$  ( $M = \text{Co}, \text{Mn}$ ). Although the  $S/T$  of the parent compound  $\text{Sr}_2\text{RuO}_4$  increases with cooling down to the lowest temperature  $\sim 3$  K similar to previous reports, for Co- and Mn-substituted systems,  $S/T$  is enhanced near  $T_w$  and  $T^\dagger$  in the irreversible magnetization. The emergence of the peak structure in  $S/T$  can be related to glassy FM and AFM fluctuations in the Co- and Mn-substituted system, respectively, and therefore the increase of  $S/T$  in  $\text{Sr}_2\text{RuO}_4$  persisting at least down to  $\sim 3$  K suggests that both FM and AFM

fluctuations seem to be substantial in  $\text{Sr}_2\text{RuO}_4$ .

The authors acknowledge Y. Maeno and K. Ishida for fruitful discussions. This work was supported by JSPS KAKENHI Grants No. JP17H06136 and No. JP18K13504.

\* takayoshi.yamanaka.b5@tohoku.ac.jp; Present address: Institute for Materials Research, Tohoku University, Sendai 980-8577, Japan

† okazaki@rs.tus.ac.jp

- [1] Y. Maeno, H. Hashimoto, K. Yoshida, S. Nishizaki, T. Fujita, J. G. Bednorz, and F. Lichtenberg, Superconductivity in a layered perovskite without copper, *Nature* **372**, 532 (1994).
- [2] T. M. Rice and M. Sigrist,  $\text{Sr}_2\text{RuO}_4$ : an electronic analogue of  $^3\text{He}$ ?, *J. Phys.: Condens. Matter* **7**, L643 (1995).
- [3] A. P. Mackenzie and Y. Maeno, The superconductivity of  $\text{Sr}_2\text{RuO}_4$  and the physics of spin-triplet pairing, *Rev. Mod. Phys.* **75**, 657 (2003).
- [4] C. Kallin, Chiral p-wave order in  $\text{Sr}_2\text{RuO}_4$ , *Rep. Prog. Phys.* **75**, 042501 (2012).
- [5] A. P. Mackenzie, T. Scaffidi, C. W. Hicks, and Y. Maeno, Even odder after twenty-three years: The superconducting order parameter puzzle of  $\text{Sr}_2\text{RuO}_4$ , *npj Quant. Mater.* **2**, 40 (2017).
- [6] S. A. Kivelson, A. C. Yuan, B. Ramshaw, and R. Thomale, A proposal for reconciling diverse experiments on the superconducting state in  $\text{Sr}_2\text{RuO}_4$ , *npj Quant. Mater.* **5**, 43 (2020).
- [7] A. Pustogow, Y. Luo, A. Chronister, Y.-S. Su, D. A. Sokolov, F. Jerzembeck, A. P. Mackenzie, C. W. Hicks, N. Kikugawa, S. Raghu, E. D. Bauer, and S. E. Brown Constraints on the superconducting order parameter in  $\text{Sr}_2\text{RuO}_4$  from oxygen-17 nuclear magnetic resonance, *Nature* **574**, 72 (2019).
- [8] K. Ishida, M. Manago, K. Kinjo, and Y. Maeno, Reduction of the  $^{17}\text{O}$  Knight Shift in the Superconducting State and the Heat-up Effect by NMR Pulses on  $\text{Sr}_2\text{RuO}_4$ , *J. Phys. Soc. Jpn.* **89**, 034712 (2020).
- [9] A. Chronister, A. Pustogow, N. Kikugawa, D. A. Sokolov, F. Jerzembeck, C. W. Hicks, A. P. Mackenzie, E. D. Bauer, and S. E. Brown, Evidence for even parity unconventional superconductivity in  $\text{Sr}_2\text{RuO}_4$ , *Proc. Natl. Acad. Sci. U.S.A.* **118**, e2025313118 (2021).
- [10] S. Kittaka, T. Nakamura, Y. Aono, S. Yonezawa, K. Ishida, and Y. Maeno, Angular dependence of the upper critical field of  $\text{Sr}_2\text{RuO}_4$ , *Phys. Rev. B* **80**, 174514 (2009).
- [11] S. Yonezawa, T. Kajikawa, and Y. Maeno, First-Order Superconducting Transition of  $\text{Sr}_2\text{RuO}_4$ , *Phys. Rev. Lett.* **110**, 077003 (2013).
- [12] C. W. Hicks, D. O. Brodsky, E. A. Yelland, A. S. Gibbs, Jan A. N. Bruin, M. E. Barber, S. D. Edkins, K. Nishimura, S. Yonezawa, Y. Maeno, and A. P. Mackenzie, Strong Increase of  $T_c$  of  $\text{Sr}_2\text{RuO}_4$  Under Both Tensile and Compressive Strain, *Science* **344**, 283 (2014).
- [13] K. Ishida, H. Mukuda, Y. Kitaoka, K. Asayama, Z. Q. Mao, Y. Mori, and Y. Maeno, Spin-triplet superconductivity in  $\text{Sr}_2\text{RuO}_4$  identified by  $^{17}\text{O}$  Knight shift, *Nature* **396**, 658 (1998).
- [14] H. Murakawa, K. Ishida, K. Kitagawa, H. Ikeda, Z. Q. Mao, and Y. Maeno,  $^{101}\text{Ru}$  Knight Shift Measurement of Superconducting  $\text{Sr}_2\text{RuO}_4$  under Small Magnetic Fields Parallel to the  $\text{RuO}_2$  Plane, *J. Phys. Soc. Jpn.* **76**, 024716 (2007).
- [15] K. Ishida, H. Murakawa, H. Mukuda, Y. Kitaoka, Z. Q. Mao, and Y. Maeno, NMR and NQR studies on superconducting  $\text{Sr}_2\text{RuO}_4$ , *J. Phys. Soc. Jpn.* **76**, 024716 (2007).
- [16] K. Ishida, M. Manago, T. Yamanaka, H. Fukazawa, Z. Q. Mao, Y. Maeno, and K. Miyake, Spin polarization enhanced by spin-triplet pairing in  $\text{Sr}_2\text{RuO}_4$  probed by NMR, *Phys. Rev. B* **92**, 100502(R) (2015).
- [17] S. Benhabib, C. Lupien, I. Paul, L. Berges, M. Dion, M. Nardone, A. Zitouni, Z. Q. Mao, Y. Maeno, A. Georges, L. Taillefer, and C. Proust Ultrasound evidence for a two-component superconducting order parameter in  $\text{Sr}_2\text{RuO}_4$ , *Nat. Phys.* **17**, 194 (2021).
- [18] S. Ghosh, A. Shekhter, F. Jerzembeck, N. Kikugawa, D. A. Sokolov, M. Brando, A. P. Mackenzie, C. W. Hicks, and B. J. Ramshaw, Thermodynamic evidence for a two-component superconducting order parameter in  $\text{Sr}_2\text{RuO}_4$ , *Nat. Phys.* **17**, 199 (2021).
- [19] V. Grinenko, S. Ghosh, R. Sarkar, J.-C. Orain, A. Nikitin, M. Elender, D. Das, Z. Guguchia, F. Brückner, M. E. Barber, J. Park, N. Kikugawa, D. A. Sokolov, J. S. Bobowski, T. Miyoshi, Y. Maeno, A. P. Mackenzie, H. Luetkens, C. W. Hicks, and H.-H. Klauss, Split superconducting and time-reversal symmetry-breaking transitions in  $\text{Sr}_2\text{RuO}_4$  under stress, *Nat. Phys.* **17**, 748 (2021).
- [20] Y. Kasahara, T. Iwasawa, H. Shishido, T. Shibauchi, K. Behnia, Y. Haga, T. D. Matsuda, Y. Onuki, M. Sigrist, and Y. Matsuda, Exotic Superconducting Properties in the Electron-Hole-Compensated Heavy-Fermion “Semimetal”  $\text{URu}_2\text{Si}_2$ , *Phys. Rev. Lett.* **99**, 116402 (2007).
- [21] M. Smidman, M. B. Salamon, H. Q. Yuan, and D. F. Agterberg, Superconductivity and spin-orbit coupling in non-centrosymmetric materials: A review, *Rep. Prog. Phys.* **80**, 036501 (2017).
- [22] O. Gingras, R. Nourafkan, A.-M. S. Tremblay, and M. Côté Superconducting Symmetries of  $\text{Sr}_2\text{RuO}_4$  from First-Principles Electronic Structure, *Phys. Rev. Lett.* **123**, 217005 (2019).
- [23] A. T. Rømer, D. D. Scherer, I. M. Eremin, P. J. Hirschfeld, and B. M. Andersen, Knight Shift and Leading Superconducting Instability from Spin Fluctuations in  $\text{Sr}_2\text{RuO}_4$ , *Phys. Rev. Lett.* **123**, 247001 (2019).
- [24] H. G. Suh, H. Menke, P. M. R. Brydon, C. Timm, A. Ramires, and D. F. Agterberg, Stabilizing even-parity chiral superconductivity in  $\text{Sr}_2\text{RuO}_4$ , *Phys. Rev. Research* **2**, 032023(R) (2020).
- [25] R. Willa, M. Hecker, R. M. Fernandes, and J. Schmalian, Inhomogeneous time-reversal symmetry breaking in  $\text{Sr}_2\text{RuO}_4$ , *Phys. Rev. B* **104**, 024511 (2021).
- [26] A. T. Rømer, P. J. Hirschfeld, and B. M. Andersen, Superconducting state of  $\text{Sr}_2\text{RuO}_4$  in the presence of longer-range Coulomb interactions, *Phys. Rev. B* **104**, 064507 (2021).
- [27] S.-J. Zhang, D. Wang, and Q.-H. Wang, Possible two-component spin-singlet pairings in  $\text{Sr}_2\text{RuO}_4$ , *Phys. Rev. B* **104**, 094504 (2021).
- [28] T. Das and C. Panagopoulos, Two types of superconducting domes in unconventional superconductors, *New J. Phys.* **18**, 103033 (2016).
- [29] S. Paschen and Q. Si, Quantum phases driven by strong correlations., *Nat. Rev. Phys.* **3**, 9-26 (2021).
- [30] A. P. Mackenzie, R. K. W. Haselwimmer, A. W. Tyler, G. G. Lonzarich, Y. Mori, S. Nishizaki, and Y. Maeno, Extremely Strong Dependence of Superconductivity on Disorder in  $\text{Sr}_2\text{RuO}_4$ , *Phys. Rev. Lett.* **80**, 161 (1998).
- [31] S. Nakatsuji and Y. Maeno, Quasi-Two-Dimensional Mott Transition System  $\text{Sr}_{2-x}\text{Ca}_x\text{RuO}_4$ , *Phys. Rev. Lett.* **84**, 2666 (2000).
- [32] J. P. Carlo, T. Goko, I. M. Gat-Malureanu, P. L. Russo, A. T. Savici, A. A. Aczel, G. J. MacDougall, J. A. Rodriguez, T. J.

- Williams, G. M. Luke, C. R. Wiebe, Y. Yoshida, S. Nakatsuji, Y. Maeno, T. Taniguchi, and Y. J. Uemura, New magnetic phase diagram of  $(\text{Sr,Ca})_2\text{RuO}_4$ , *Nat. Mater.* **11**, 323 (2012).
- [33] M. Minakata and Y. Maeno, Magnetic ordering in  $\text{Sr}_2\text{RuO}_4$  induced by nonmagnetic impurities, *Phys. Rev. B* **63**, 180504(R) (2001).
- [34] N. Kikugawa, A. P. Mackenzie, C. Bergemann, R. A. Borzi, S. A. Grigera, and Y. Maeno, Rigid-band shift of the Fermi level in the strongly correlated metal:  $\text{Sr}_{2-y}\text{La}_y\text{RuO}_4$ , *Phys. Rev. B* **70**, 060508(R) (2004).
- [35] N. Kikugawa, C. Bergemann, A. P. Mackenzie, and Y. Maeno, Band-selective modification of the magnetic fluctuations in  $\text{Sr}_2\text{RuO}_4$ : A study of substitution effects, *Phys. Rev. B* **70**, 134520 (2004).
- [36] K. M. Shen, N. Kikugawa, C. Bergemann, L. Balicas, F. Baumberger, W. Meevasana, N. J. C. Ingle, Y. Maeno, Z.-X. Shen, and A. P. Mackenzie, Evolution of the Fermi Surface and Quasiparticle Renormalization through a van Hove Singularity in  $\text{Sr}_{2-y}\text{La}_y\text{RuO}_4$ , *Phys. Rev. Lett.* **99**, 187001 (2007).
- [37] T. Imai, A. W. Hunt, K. R. Thurber, and F. C. Chou,  $^{17}\text{O}$  NMR Evidence for Orbital Dependent Ferromagnetic Correlations in  $\text{Sr}_2\text{RuO}_4$ , *Phys. Rev. Lett.* **81**, 3006 (1998).
- [38] Y. Sidis, M. Braden, P. Bourges, B. Hennion, S. Nishizaki, Y. Maeno, and Y. Mori, Evidence for Incommensurate Spin Fluctuations in  $\text{Sr}_2\text{RuO}_4$ , *Phys. Rev. Lett.* **83**, 3320 (1999).
- [39] M. Braden, Y. Sidis, P. Bourges, P. Pfeuty, J. Kulda, Z. Mao, and Y. Maeno, Inelastic neutron scattering study of magnetic excitations in  $\text{Sr}_2\text{RuO}_4$ , *Phys. Rev. B* **66**, 064522 (2002).
- [40] P. Steffens, Y. Sidis, J. Kulda, Z. Q. Mao, Y. Maeno, I. I. Mazin, and M. Braden, Spin Fluctuations in  $\text{Sr}_2\text{RuO}_4$  from Polarized Neutron Scattering: Implications for Superconductivity, *Phys. Rev. Lett.* **122**, 047004 (2019).
- [41] K. Jenni, S. Kunkemöller, P. Steffens, Y. Sidis, R. Bewley, Z. Q. Mao, Y. Maeno, and M. Braden, Neutron scattering studies on spin fluctuations in  $\text{Sr}_2\text{RuO}_4$ , *Phys. Rev. B* **103**, 104511 (2021).
- [42] J. E. Ortmann, J. Y. Liu, J. Hu, M. Zhu, J. Peng, M. Matsuda, X. Ke, and Z. Q. Mao, Competition Between Antiferromagnetism and Ferromagnetism in  $\text{Sr}_2\text{RuO}_4$  Probed by Mn and Co Doping, *Sci. Rep.* **3**, 2950 (2013).
- [43] K. Behnia, *Fundamentals of Thermoelectricity*, Oxford University Press (2015).
- [44] Z. Q. Mao, Y. Maeno, and H. Fukazawa, Crystal growth of  $\text{Sr}_2\text{RuO}_4$ , *Mater. Res. Bull.* **35**, 1813 (2000).
- [45] H. Yoshino, K. Murata, N. Shirakawa, Y. Nishihara, Y. Maeno, and T. Fujita, Thermopower of a Layered Perovskite Superconductor,  $\text{Sr}_2\text{RuO}_4$ , *J. Phys. Soc. Jpn.* **65**, 1548 (1996).
- [46] X. F. Xu, Z. A. Xu, T. J. Liu, D. Fobes, Z. Q. Mao, J. L. Luo, and Y. Liu, Band-Dependent Normal-State Coherence in  $\text{Sr}_2\text{RuO}_4$ : Evidence from Nernst Effect and Thermopower Measurements, *Phys. Rev. Lett.* **101**, 057002 (2008).
- [47] J. Mravlje and A. Georges, Thermopower and Entropy: Lessons from  $\text{Sr}_2\text{RuO}_4$ , *Phys. Rev. Lett.* **117**, 036401 (2016).
- [48] J. Mravlje, M. Aichhorn, T. Miyake, K. Haule, G. Kotliar, and A. Georges, Coherence-Incoherence Crossover and the Mass-Renormalization Puzzles in  $\text{Sr}_2\text{RuO}_4$ , *Phys. Rev. Lett.* **106**, 096401 (2011).
- [49] R. Okazaki, A. Horikawa, Y. Yasui, and I. Terasaki, Photo-Seebeck Effect in  $\text{ZnO}$ , *J. Phys. Soc. Jpn.* **81**, 114722 (2012).
- [50] K. Behnia, D. Jaccard, and J. Flouquet, On the thermoelectricity of correlated electrons in the zero-temperature limit, *J. Phys.: Condens. Matter* **16**, 5187 (2004).
- [51] I. Terasaki, Cobalt Oxides and Kondo Semiconductors: A Pseudogap System as a Thermoelectric Material, *Mater. Trans.* **42**, 951 (2001).
- [52] Y. Ikeda, K. Saito, and R. Okazaki, Thermoelectric transport in the layered  $\text{Ca}_3\text{Co}_{4-x}\text{Rh}_x\text{O}_9$  single crystals, *J. Appl. Phys.* **119**, 225105 (2016).
- [53] C. Collignon, A. Ataei, A. Gourgout, S. Badoux, M. Lizaire, A. Legros, S. Licciardello, S. Wiedmann, J.-Q. Yan, J.-S. Zhou, Q. Ma, B. D. Gaulin, N. Doiron-Leyraud, and L. Taillefer, Thermopower across the phase diagram of the cuprate  $\text{La}_{1.6-x}\text{Nd}_{0.4}\text{Sr}_x\text{CuO}_4$ : Signatures of the pseudogap and charge density wave phases, *Phys. Rev. B* **103**, 155102 (2021).
- [54] V. Zlatić, B. Horvatić, I. Milat, B. Coqblin, G. Czycholl, and C. Grenzbach, Thermoelectric power of cerium and ytterbium intermetallics, *Phys. Rev. B* **68**, 104432 (2003).
- [55] K. Kurita, H. Sakabayashi, and R. Okazaki, Correlation in transport coefficients of hole-doped  $\text{CuRhO}_2$  single crystals, *Phys. Rev. B* **99**, 115103 (2019).
- [56] C. Pappa, J. Hammann and C. Jacoboni, Spin-glass-like H-T phase diagram for the frustrated insulator  $\text{CsNiFeF}_6$ , *J. Phys. C: Solid State Phys.* **17**, 1303 (1984).
- [57] G. C. DeFotis, G. S. Coker, J. W. Jones, C. S. Branch, H. A. King, J. S. Bergman, S. Lee, and J. R. Goodey, Static magnetic properties and relaxation of the insulating spin glass  $\text{Co}_{1-x}\text{Mn}_x\text{Cl}_2 \cdot \text{H}_2\text{O}$ , *Phys. Rev. B* **58**, 12178 (1998).
- [58] S. Dhar, O. Brandt, A. Trampert, K. J. Friedland, Y. J. Sun, and K. H. Ploog, Observation of spin-glass behavior in homogeneous  $(\text{Ga,Mn})\text{N}$  layers grown by reactive molecular-beam epitaxy, *Phys. Rev. B* **67**, 165205 (2003).
- [59] J. Lago, S. J. Blundell, A. Eguia, M. Jansen, and T. Rojo, Three-dimensional Heisenberg spin-glass behavior in  $\text{SrFe}_{0.90}\text{Co}_{0.10}\text{O}_{3.0}$ , *Phys. Rev. B* **86**, 064412 (2012).
- [60] M. Gabay, and G. Toulouse, Coexistence of Spin-Glass and Ferromagnetic Orderings, *Phys. Rev. Lett.* **47**, 201 (1981).
- [61] T. D. Yamamoto, H. Taniguchi, Y. Yasui, S. Iguchi, T. Sasaki, and I. Terasaki, Magneto-thermopower in the Weak Ferromagnetic Oxide  $\text{CaRu}_{0.8}\text{Sc}_{0.2}\text{O}_3$ : An Experimental Test for the Kelvin Formula in a Magnetic Material, *J. Phys. Soc. Jpn.* **86**, 104707 (2017).
- [62] N. Tsujii, A. Nishide, J. Hayakawa, and T. Mori, Observation of enhanced thermopower due to spin fluctuation in weak itinerant ferromagnet, *Sci. Adv.* **5**, eaat5935 (2019).
- [63] T. Ikeura, T. Matsubara, Y. Machida, K. Izawa, N. Nagasawa, K. T. Matsumoto, T. Onimaru, and T. Takabatake, Anomalous Enhancement of Seebeck Coefficient in  $\text{PrIr}_2\text{Zn}_2\text{O}$ , *JPS Conf. Proc.* **3**, 011091 (2014).
- [64] D. K. C. Macdonald, W. B. Pearson, and I. M. Templeton, Thermo-electricity at low temperatures VIII. Thermoelectricity of the alkali metals below 2 K, *Proc. Royal Soc. London A*, **256**, 334 (1960).
- [65] I. Paul and G. Kotliar, Thermoelectric behavior near the magnetic quantum critical point, *Phys. Rev. B* **64**, 184414 (2001).
- [66] K. Izawa, K. Behnia, Y. Matsuda, H. Shishido, R. Settai, Y. Onuki, and J. Flouquet, Thermoelectric Response Near a Quantum Critical Point: The Case of  $\text{CeCoIn}_5$ , *Phys. Rev. Lett.* **99**, 147005 (2007).
- [67] S. Hartmann, N. Oeschler, C. Krellner, C. Geibel, S. Paschen, and F. Steglich, Thermopower Evidence for an Abrupt Fermi Surface Change at the Quantum Critical Point of  $\text{YbRh}_2\text{Si}_2$ , *Phys. Rev. Lett.* **104**, 096401 (2010).
- [68] L. Malone, L. Howald, A. Pourret, D. Aoki, V. Taufour, G. Knebel, and J. Flouquet, Thermoelectricity of the ferromagnetic superconductor  $\text{UCoGe}$ , *Phys. Rev. B* **85**, 024526 (2012).
- [69] H. Pfau, R. Daou, M. Brando, and F. Steglich, Thermoelectric transport across the metamagnetic transition of  $\text{CeRu}_2\text{Si}_2$ , *Phys. Rev. B* **85**, 035127 (2012).

- [70] Y. Shimizu, A. Pourret, G. Knebel, A. Palacio-Morales, and D. Aoki, Non-Fermi-liquid nature and exotic thermoelectric power in the heavy-fermion superconductor  $\text{URu}_2\text{Si}_2$ , *Phys. Rev. B* **92**, 241101(R) (2015).
- [71] P. Limelette, W. Saulquin, H. Muguerra, and D. Grebille, From quantum criticality to enhanced thermopower in strongly correlated layered cobalt oxide, *Phys. Rev. B* **81**, 115113 (2010).
- [72] Y. Maeno, K. Yoshida, H. Hashimoto, S. Nishizaki, S. Ikeda, M. Nohara, T. Fujita, A. P. Mackenzie, N. E. Hussey, J. G. Bednorz, and F. Lichtenberg, Two-Dimensional Fermi Liquid Behavior of the Superconductor  $\text{Sr}_2\text{RuO}_4$ , *J. Phys. Soc. Jpn.* **66**, 1405 (1997).
- [73] K.-S. Kim and C. Pépin, Thermopower as a signature of quantum criticality in heavy fermions, *Phys. Rev. B* **81**, 205108 (2010).
- [74] K. Miyake and H. Kohno, Theory of Quasi-Universal Ratio of Seebeck Coefficient to Specific Heat in Zero-Temperature Limit in Correlated Metals, *J. Phys. Soc. Jpn.* **74**, 254 (2005).
- [75] T. Oguchi, Electronic band structure of the superconductor  $\text{Sr}_2\text{RuO}_4$ , *Phys. Rev. B* **51**, 1385 (1995).
- [76] D. J. Singh, Relationship of  $\text{Sr}_2\text{RuO}_4$  to the superconducting layered cuprates, *Phys. Rev. B* **52**, 1358 (1995).
- [77] A. P. Mackenzie, S. R. Julian, A. J. Diver, G. J. McMullan, M. P. Ray, G. G. Lonzarich, Y. Maeno, S. Nishizaki, and T. Fujita, Quantum Oscillations in the Layered Perovskite Superconductor  $\text{Sr}_2\text{RuO}_4$ , *Phys. Rev. Lett.* **76**, 3786 (1996).
- [78] S. Hill, J. S. Brooks, Z. Q. Mao, and Y. Maeno, Cyclotron resonance and effective mass renormalizations in  $\text{Sr}_2\text{RuO}_4$ , *Physica B* **280**, 283 (2000).
- [79] K. Yano, T. Sakakibara, T. Tayama, M. Yokoyama, H. Amitsuka, Y. Homma, P. Miranović, M. Ichioka, Y. Tsutsumi, and K. Machida, Field-Angle-Dependent Specific Heat Measurements and Gap Determination of a Heavy Fermion Superconductor  $\text{URu}_2\text{Si}_2$ , *Phys. Rev. Lett.* **100**, 017004 (2008).
- [80] N. Kikugawa and Y. Maeno, Non-Fermi-Liquid Behavior in  $\text{Sr}_2\text{RuO}_4$  with Nonmagnetic Impurities, *Phys. Rev. Lett.* **89**, 117001 (2002).
- [81] N. Tateiwa, T. D. Matsuda, Y. Ōnuki, Y. Haga, and Z. Fisk, Strong correlation between anomalous quasiparticle scattering and unconventional superconductivity in the hidden-order phase of  $\text{URu}_2\text{Si}_2$ , *Phys. Rev. B* **85**, 054516 (2012).
- [82] J. S. Bobowski, N. Kikugawa, T. Miyoshi, H. Suwa, H.-s. Xu, S. Yonezawa, D. A. Sokolov, A. P. Mackenzie, and Y. Maeno, Improved Single-Crystal Growth of  $\text{Sr}_2\text{RuO}_4$ , *Condens. Matter* **4**, 6 (2019).
- [83] M. A. Tanatar, M. Suzuki, S. Nagai, Z. Q. Mao, Y. Maeno, and T. Ishiguro, Anisotropy of Magnetothermal Conductivity in  $\text{Sr}_2\text{RuO}_4$ , *Phys. Rev. Lett.* **86**, 2649 (2001).
- [84] K. Izawa, H. Takahashi, H. Yamaguchi, Yuji Matsuda, M. Suzuki, T. Sasaki, T. Fukase, Y. Yoshida, R. Settai, and Y. Onuki, Superconducting Gap Structure of Spin-Triplet Superconductor  $\text{Sr}_2\text{RuO}_4$  Studied by Thermal Conductivity, *Phys. Rev. Lett.* **86**, 2653 (2001).
- [85] M. Suzuki, M. A. Tanatar, N. Kikugawa, Z. Q. Mao, Y. Maeno, and T. Ishiguro, Universal Heat Transport in  $\text{Sr}_2\text{RuO}_4$ , *Phys. Rev. Lett.* **88**, 227004 (2002).
- [86] A. A. Varlamov, V. S. Egorov, and A. V. Pantsulaya, Kinetic properties of metals near electronic topological transitions (2 1/2-order transitions), *Adv. Phys.* **38**, 469 (1989).
- [87] N. Ito, M. Ishii, and R. Okazaki, Enhanced Seebeck coefficient by a filling-induced Lifshitz transition in  $\text{K}_x\text{RhO}_2$ , *Phys. Rev. B* **99**, 041112(R) (2019).